

Double Giant Dipole Resonance in ^{208}Pb

S. NISHIZAKI

*Faculty of Humanities and Social Sciences, Iwate University,
3-18-34 Ueda, Morioka 020, Japan*

J. Wambach

*Institut für Kernphysik, Technische Hochschule Darmstadt,
Schlossgartenstrasse 9, D-64289 Darmstadt, Germany*

Double-dipole excitations in ^{208}Pb are analyzed within a microscopic model explicitly treating 2p2h-excitations. Collective states built from such 2p2h-excitations are shown to appear at about twice the energy of the isovector giant dipole resonance, in agreement with the experimental findings. The calculated cross section for Coulomb excitation at relativistic energies cannot explain simultaneously the measured single-dipole and double-dipole cross sections, however.

1 Introduction

Double giant dipole resonances (DGDR) have been observed in pion double-charge-exchange reactions at LAMPF [1] as well as in high-energy heavy-ion collisions at GSI [2]. In the latter case there is a strong focusing of the electromagnetic field in the target rest frame. This greatly enhances the field intensity in the vicinity of the target nucleus, thus increasing the probability for two-photon absorption from the ground state.

The global parameters of the DGDR, *i.e.* the resonance energy E_{DGDR} , the width Γ_{DGDR} and the cross section σ can be summarized as follows [3]: 1) The resonance energy is about twice as large as that of the isovector giant dipole resonance (GDR), $E_{DGDR} \simeq 2E_{GDR}$. which suggests that can be interpreted as an independent two-phonon state. 2) The observed values of the width Γ_{DGDR} are bracketed by $\sqrt{2}\Gamma_{GDR}$ and $2\Gamma_{GDR}$. Also this feature supports a harmonic picture. 3) The measured cross section σ_{exp} is larger than the theoretical estimate σ_{th} . The values of the ratio $\sigma_{\text{exp}}/\sigma_{\text{th}}$ are scattered between 1 and 5 depending on the nuclei considered and on the theoretical analyses. This puts into some doubt to interpret the DGDR as an independent two-phonon state.

To reach a quantitative understanding of the DGDR characteristics we shall carry out a microscopic calculation of the DGDR in ^{208}Pb . The structure of double-dipole states are investigated by the diagonalization of a model Hamiltonian in the space of 1p1h- and 2p2h-excitations. For comparison with experiment the cross section for Coulomb excitation, based on the second-order perturbation theory, will be estimated.

2 Double-Dipole Strength Distribution in ^{208}Pb

2.1 Microscopic Model

The nuclear structure model has been developed in our previous work [4] on double-dipole excitations in ^{40}Ca . We give a brief outline stressing some new aspects in the application to heavy nuclei such as ^{208}Pb . The eigenstates $|n\rangle$ of the nuclear Hamiltonian \hat{H}_0 are

determined by diagonalizing \hat{H}_0 in the space of 1p1h- and 2p2h-excitations. As a model space of single-particle states, we take into account three major shells of the Woods-Saxon potential on both sides of the Fermi level. The continuum states are treated by discretization through an expansion in a harmonic oscillator basis. The number of 2p2h states constructed with these single-particle states exceeds several hundreds of thousand. Most of them, however, have vanishingly small matrix elements for the double-dipole transition from the ground state. Thus we select only those 2p2h-states whose energy is below 40 MeV, and which exceed a lower limit in the magnitude of the double-dipole matrix element,

$$|\langle 2p2h|\hat{D}\hat{D}|0\rangle|^2 / \sum_2 |\langle 2|\hat{D}\hat{D}|0\rangle|^2 \geq 5 \times 10^{-5}. \quad (1)$$

Here, the isovector dipole operator, \hat{D} , is defined as

$$\hat{D} = e \frac{N}{A} \sum_{i=1}^Z \mathbf{r}_i - e \frac{Z}{A} \sum_{i=1}^N \mathbf{r}_i. \quad (2)$$

With these conditions, we can reduce the number of 2p2h-states to 996 for the $J^\pi = 0^+$ double-dipole transition and to 2011 for the 2^+ transition.

The mean energy and total strength of the GDR in ^{208}Pb , calculated in the usual 1p1h-RPA with the nuclear Hamiltonian [4], including a density-dependent zero-range interaction, are 10.3 MeV and 98% of the TRK sum-rule value, respectively. Both are smaller than photo-neutron data [5] which yield 13.4 MeV and 134%. Therefore we enhance the theoretical results by a scaling of the single-particle energies according to $\varepsilon_{sp} = \varepsilon_{WS}/(m^*/m)$ with the effective mass $m^*/m = 0.75$. By this procedure, we obtain the mean energy and the total strength as 13.5 MeV and 131% of the TRK value, in good agreement with experiment.

2.2 Strength Distribution

The strength distributions of the double-dipole transition are shown in Fig. 1. Figs. 1(a) and 1(b) (1(c) and 1(d)) represent the unperturbed and the perturbed strength distributions for the 0^+ (2^+) double-dipole transitions, respectively. Both for 0^+ and 2^+ double-dipole transitions, the perturbed strength concentrates in the region of 25–30 MeV. There appear several states which carry about ten times more strength than the strongest unperturbed ones.

The mean energy, $\langle E \rangle$, and the width, Γ , are estimated in terms of the energy moments

$$m_{DD}^k = \int dE E^k S_{DD}(E), \quad S_{DD} = \sum_n |\langle n|\hat{D}\hat{D}|0\rangle|^2 \delta(E - E_n), \quad (3)$$

as

$$\langle E \rangle_{DGDR} = m_{DD}^1 / m_{DD}^0 \quad \text{and} \quad \Gamma_{DGDR} = \sqrt{m_{DD}^2 m_{DD}^0 - (m_{DD}^1)^2} / m_{DD}^0, \quad (4)$$

and similarly for the isovector dipole excitations. The $\langle E \rangle_{DGDR}$ and Γ_{DGDR} are 26.96 MeV (26.53 MeV) and 3.48 MeV (3.36 MeV) for 0^+ DGDR (2^+ DGDR), respectively.

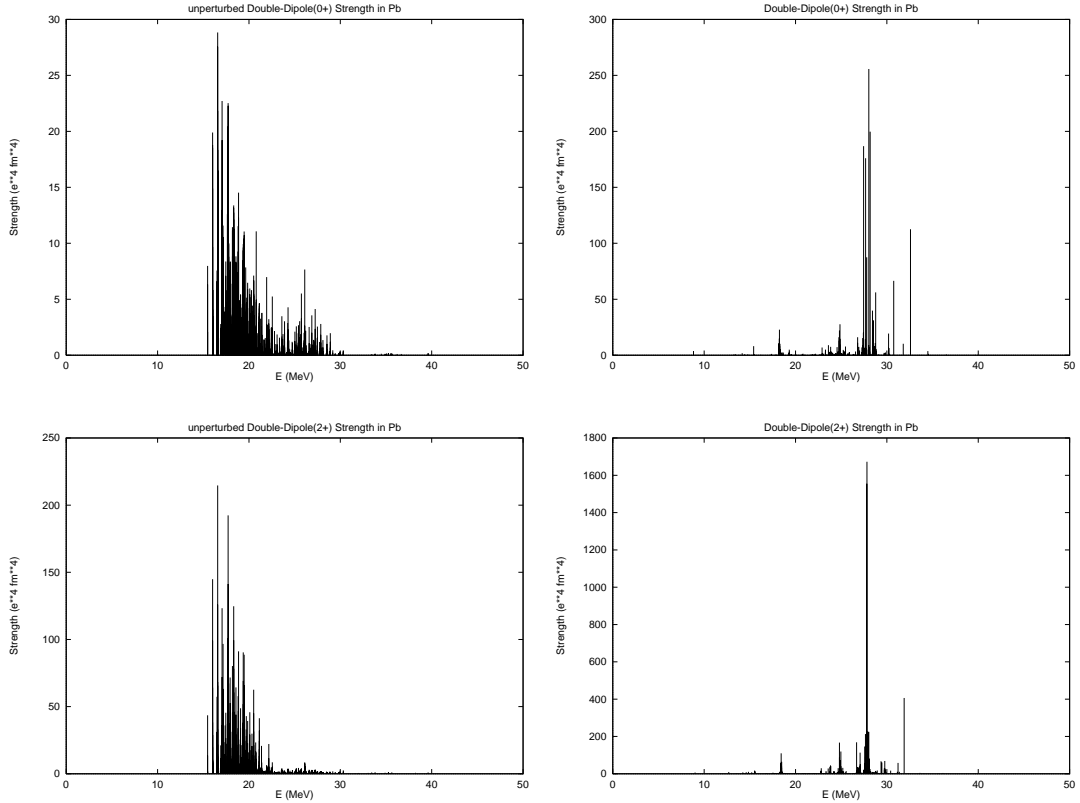


Figure 1: Double-Dipole Strength Distributions. (a) Unperturbed 0^+ DD strength. (b) Perturbed 0^+ DD strength. (c) Unperturbed 2^+ DD strength. (d) Perturbed 2^+ DD strength.

The mean energy of the DGDR is about twice as large as that of the GDR. The calculated width, which corresponds to the fragmentation width (Landau damping) is larger than that of the GDR ($\Gamma_{GDR} = 2.70$ MeV) by the factor of 1.24–1.29. We note that the observed width includes, in addition, the escaping and spreading width which are not included in the present calculation.

3 Cross Section for the Coulomb Excitation

3.1 Second-order Coulomb-Excitation Amplitude

In the semiclassical approach [6,7], the cross section for Coulomb excitation is given by

$$\sigma_{i \rightarrow f} = 2\pi \int_{R_{min}}^{\infty} b db \frac{1}{2J_i + 1} \sum_{M_i, M_f} |a_{fi}|^2. \quad (5)$$

The projectile is assumed to move on a straight-line trajectory with impact parameter b . The minimum impact parameter R_{min} is a key parameter, since the cross section sensitively depends on it as will be shown later.

The main components of the DGDR are 2p2h-states, which are excited via a two-body operator of double-dipole character ($\hat{D}\hat{D}$) from the ground state. For Coulomb excitation the precise form of the excitation operator is derived from the 2nd-order amplitude

$$a_{fi}^{(2)} = \frac{1}{(i\hbar)^2} \langle f | \int_{-\infty}^{+\infty} dt \int_{-\infty}^t dt' e^{+i\hat{H}_0 t/\hbar} \hat{V}(t) e^{-i\hat{H}_0 t/\hbar} e^{+i\hat{H}_0 t'/\hbar} \hat{V}(t') e^{-i\hat{H}_0 t'/\hbar} | i \rangle, \quad (6)$$

where \hat{H}_0 and \hat{V} are the nuclear Hamiltonian and the Coulomb interaction between the projectile and target nuclei, respectively. To obtain the two-body operator, we exchange the order of $\hat{V}(t)$ ($\hat{V}(t')$) and $\exp(+i\hat{H}_0 t'/\hbar)$ ($\exp(-i\hat{H}_0 t/\hbar)$). This yields a series expansion in the times t and t' which includes single- and multiple-commutators of \hat{H}_0 and \hat{V} . In the limit of a 'fast collision' [8], we need only to take into account the lowest order in time. Finally the expression for the second-order amplitude of the double $E\lambda'$ transition is given by

$$\begin{aligned} a_{fi}^{(2)} &= (4\pi \frac{Ze}{i\hbar})^2 \sum_{\mu} \frac{(-)^{\mu}}{(2\lambda' + 1)^2} \\ &\times \left\{ \frac{1}{2} \langle f | \mathcal{N}_{EE}^{\lambda'\lambda'}(\lambda, -\mu) | i \rangle \langle T_{\lambda\mu}^{E\lambda'E\lambda'}(\omega, \omega) + \hbar\omega U_{\lambda\mu}^{E\lambda'E\lambda'}(\omega, \omega) \right. \\ &\quad \left. + \langle f | \mathcal{K}_{EE}^{\lambda'\lambda'}(\lambda, -\mu) | i \rangle \frac{i}{2\pi} \mathcal{P} \int_{-\infty}^{+\infty} \frac{dq}{q} U_{\lambda\mu}^{E\lambda'E\lambda'}(\omega - q, \omega + q) \right\}, \quad (7) \end{aligned}$$

with

$$T_{\lambda\mu}^{\pi_1\lambda_1\pi_2\lambda_2}(\omega_1, \omega_2) = [S_{\pi_1\lambda_1}(\omega_1) \otimes S_{\pi_2\lambda_2}(\omega_2)]_{\lambda\mu} \quad (8)$$

$$U_{\lambda\mu}^{\pi_1\lambda_1\pi_2\lambda_2}(\omega_1, \omega_2) = [S_{\pi_1\lambda_1}(\omega_1) \otimes R_{\pi_2\lambda_2}(\omega_2)]_{\lambda\mu} \quad (9)$$

$$\mathcal{N}_{\pi_1\pi_2}^{\lambda_1\lambda_2}(\lambda, \mu) = [\mathcal{M}(\pi_1\lambda_1) \otimes \mathcal{M}(\pi_2\lambda_2)]_{\lambda\mu} \quad (10)$$

$$\begin{aligned} \mathcal{K}_{\pi_1\pi_2}^{\lambda_1\lambda_2}(\lambda, \mu) &= [[H_0, \mathcal{M}(\pi_1\lambda_1)] \otimes \mathcal{M}(\pi_2\lambda_2) \\ &\quad - \mathcal{M}(\pi_1\lambda_1) \otimes [H_0, \mathcal{M}(\pi_2\lambda_2)]]_{\lambda\mu}. \quad (11) \end{aligned}$$

Here, $\mathcal{M}(\pi\lambda)$ denotes electric ($\pi = E$) or magnetic ($\pi = M$) multipole operators while $S_{\pi\lambda}$ and $R_{\pi\lambda}$ are orbital integrals [8]. The principal value integral in Eq. 7 results from a step function, which appears when the upper limit of the integral in Eq. 6 is extended to infinity. In the present estimate of the cross section, we neglect this principal value integral.

3.2 Cross Section

The calculated cross section for Coulomb excitation of the DGDR with a ^{208}Pb projectile incident on a Pb target at 640 MeV/A is plotted as the solid line in Fig. 2. The dashed and dotted lines display the cross sections for the GDR and the GQR (giant quadrupole resonance), respectively. For comparison the former has been multiplied by the factor

of 0.1. To account for experimental energy resolution, the calculated cross sections have been smoothed by using a Breit-Wigner function of width 1.5 MeV. The main peak of the DGDR appears in the region of 25 – 30 MeV, just above the broad isovector GQR around 20 MeV. The peak energy of the DGDR is about twice that of the GDR.

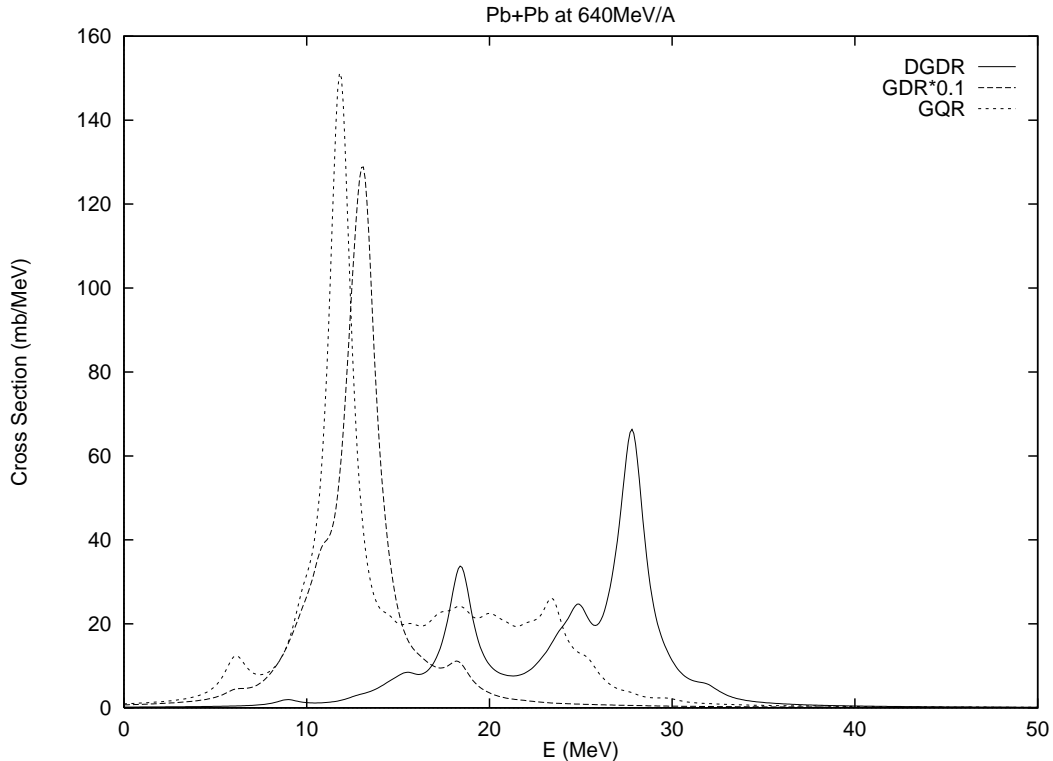


Figure 2: Cross Section for the Coulomb Excitation. The solid line denotes the cross section of the DGDR while the dashed line displays the GDR cross section (multiplied by 0.1). In addition, the cross section for the GQR is shown as the dotted line. The minimum impact parameter is the value of case (b) (see text).

Next we discuss the dependence of the energy-integrated cross section on the minimum impact-parameter, R_{min} . We parameterize R_{min} as $R_{min} = r_0(A_t^{1/3} + A_p^{1/3})$, where A_t and A_p denote the mass number of target and projectile nuclei, respectively. Three cases are considered : (a) $r_0 = 1.50$ fm, (b) $r_0 = 1.31$ fm and (c) $r_0 = 1.20$ fm. The values for (a) and (c) have been used previously by Ponomarev et al. [10] in the study of the DGDR in ^{136}Xe , while case (b) represents the choice of Boretzky et al. [9] (Fig. 2 corresponds to case (b)). The cross sections of the GDR and the DGDR in ^{208}Pb incident on various nuclei are given in Table 1 where the three cases for R_{min} are compared with the measured cross sections [9]. The intermediate value of R_{min} (case (b)) reproduces the measured cross sections of the DGDR fairly well, but overestimates those of the GDR. On the other hand, the larger value (case (a)) reproduces the measured cross sections of GDR, while underestimating those of the DGDR by the factor 2 – 3. In our

calculation it seems impossible to simultaneously explain the measured GDR and DGDR cross sections with the same value of R_{min} .

In the particle-vibration coupling calculation of the DGDR in ^{136}Xe by Ponomarev et al. [10], similar results for the cross section were obtained, but the discrepancy between the measured cross section and their estimate is larger than that in our results. On the other hand, the simple folding model analysis of the DGDR in ^{208}Pb by Boretzky et al. [9] predicts only a 33% enhancement of the DGDR cross section while reproducing the GDR cross section. It remains an open question whether this difference between results from the microscopic models and the folding model originates from the nuclear structure or from the treatment of the reaction mechanism.

Table 1: Cross section for Coulomb excitation of the GDR and DGDR in a ^{208}Pb projectile incident on U, Pb, Ho and Sn targets at 640 MeV/A.

Cross Section (b)	U		Pb		Ho		Sn	
	GDR	DGDR	GDR	DGDR	GDR	DGRD	GDR	DGDR
(a)	4.18	0.222	3.47	0.162	2.49	0.091	1.52	0.038
(b)	5.34	0.500	4.42	0.361	3.16	0.201	1.91	0.083
(c)	6.22	0.827	5.12	0.590	3.63	0.321	2.18	0.129
exp	3.66	0.51	3.28	0.38	2.47	0.28	1.45	0.07

4 Summary

We have carried out a microscopic calculation of double-dipole excitations in ^{208}Pb in a realistic model space of 1p1h- and 2p2h-states. Since the number of 2p2h-states in heavy nuclei such as ^{208}Pb , is prohibitively large we have introduced the selection procedure given by Eq. 1 as well as a truncation in the 2p2h energy. Although the width of DGDR may not be totally reliable because of this procedure, we believe that both the mean energy and the integrated strength are realistic.

The double-dipole strength is shown to be concentrated in an energy region twice that of the isovector giant dipole resonance thus indicating that anharmonicity effects are quite small, in good agreement with experiment.

The Coulomb excitation cross section has been calculated based on the second-order perturbation. It depends sensitively on the minimum impact parameter, which appears in the semiclassical treatment of the cross section for Coulomb excitation. We have estimated the cross section of the GDR and DGDR with three choices for the minimum impact parameter, available from the literature. None of these choices can explain the measured cross sections simultaneously and hence the discrepancy between the measured cross section and theoretical estimates, previously observed, remains.

Acknowledgments

We thank G. Baur and H. Emling for fruitful discussions.

References

1. S. Mordechai *et al*, *Phys. Rev. Lett.* **60**, 408 (1988) ; **61**, 531 (1988).
2. J. Ritman *et al*, *Phys. Rev. Lett.* **70**, 533 (1993).
R. Schmidt *et al*, *Phys. Rev. Lett.* **70**, 1767 (1993).
T. Aumann *et al*, *Phys. Rev. C* **47**, 1728 (1993).
3. H. Emling, *Prog. Part. Nucl. Phys.* **33**, 729 (1994).
Ph. Chomaz and N. Frascaria, *Phys. Rep.* **252**, 275 (1995).
4. S. Nishizaki and J. Wambach, *Phys. Lett. B* **349**, 7 (1995).
5. S. Veyssiere *et al*, *Nucl. Phys. A* **159**, 561 (1970).
6. A. Winter and K. Alder, *Nucl. Phys. A* **319**, 518 (1979).
K. Alder and A. Winter, *Coulomb Excitation*, (Academic Press, New York and London, 1966).
7. C.A. Bertulani and G. Baur, *Phys. Rep.* **163**, 299 (1988).
8. S. Typel and G. Baur, *Phys. Rev. C* **50**, 2104 (1994).
9. K. Boretzky *et al*, *Phys. Lett. B* **384**, 30 (1996).
10. V.Yu. Ponomarev *et al*, *Phys. Rev. Lett.* **72**, 1168 (1994).